CrossMark

Prediction of Bending Fatigue Life of Cracked Out-of-Plane Gusset Joint Repaired by CFRP Plates

Risa Matsumoto[1] · Takafumi Komoto[2] · Toshiyuki Ishikawa[3] · Atsushi Hattori[1] · Hirotaka Kawano[1]

Abstract

Carbon fiber reinforced polymer (CFRP), plates bonding repair method is one of the simple repair methods for cracked steel structures. In this study, the influence of width of CFRP plates on bending fatigue life of out-of-plane gusset joint strengthened with CFRP plates was investigated from the experimental and numerical point of view. In the bending fatigue test of cracked out-of-plane gusset joint strengthened with CFRP plates, the effect of width of CFRP plates on crack growth life was clarified experimentally. Namely, it was revealed that the crack growth life becomes larger with increasing the width of CFRP plates. In the numerical approach, the stress intensity factor (*SIF*) at the surface point of a semi-elliptical surface crack was estimated based on the linear fracture mechanics. Furthermore, the extended fatigue life of cracked out-of-plane gusset joint strengthened with CFRP plates was evaluated by using the estimated *SIF* at the surface point and the empirical formula of the aspect ratio of semi-elliptical crack. As the results of numerical analysis, the estimated fatigue life of the specimen strengthened with CFRP plates showed the good agreement with the test results.

Keywords CFRP plate · Out-of-plane gusset joint · Bending moment · Stress intensity factor · Linear fracture mechanics

1 Introduction

Carbon fiber reinforced plastic, CFRP, plates bonding repair method has been studied as the repair method for corroded steel structures or cracked steel structures, and employed as the repair method for the existing corroded steel structures

✉ Risa Matsumoto
 Matsumoto.risa.8z@kyoto-u.ac.jp

 Takafumi Komoto
 t.komoto1714@shutoko.jp

 Toshiyuki Ishikawa
 t-ishi@kansai-u.ac.j

 Atsushi Hattori
 hattori.atsushi.7z@kyoto-u.ac.jp

 Hirotaka Kawano
 kawano.hirotaka.8n@kyoto-u.ac.jp

[1] Department of Urban Management, Kyoto University, Kyotodaigaku-katsura, Nishikyo-ku, Kyoto 615-8540, Japan

[2] Metropolitan Expressway Company, 1-4-1 Kasumigaseki, Chiyoda-ku, Tokyo 100-0013, Japan

[3] Department of Civil, Environmental, and Applied System Engineering, Kansai University, 3-3-35 Suita-shi Yamate-cho, Osaka 564-8680, Japan

(e.g. National Research Council 2007; Chacon et al. 2004; Phares et al. 2003; Roach et al. 2008). The CFRP plate has excellent material properties with lower weight, and applicability to rapid repairs. In order to spread the bonding technique of CFRP plates as crack repair method for the existing steel bridge, it is important to predict the crack growth life of steel member strengthened with CFRP plates quantitatively.

Since the crack growth rate depends on the stress intensity factor (*SIF*), the previous studies have been focused on the reduction of *SIF* to predict the extended fatigue life of a cracked steel plate strengthened with CFRP plates quantitatively. In particular, some of them predicted the extended fatigue life of cracked steel plate repaired by bonding CFRP plate focused on *SIF*s under axial loading condition. For instance, Ye et al. (2010) investigated the fatigue life performance on tension steel plates strengthened with pre-stressed CFRP laminates. Wang et al. (2013) revealed the effect of FRP configurations on the extended fatigue life. Colombi et al. (2015) investigated the fatigue crack growth in CFRP-strengthened steel plates with edge crack. However, they were evaluated the crack growth life of a steel plate strengthened with CFRP plates from single aspect, i.e. experimental results or FE analysis, Some researchers have been proposed the equation of the *SIF* of cracked plate reinforced with

CFRP plates considering the dimensions of CFRP plates, the stiffness of CFRP plates and bonding position, and the extended fatigue life of cracked steel plate strengthened with CFRP plates was satisfactorily predicted by using the proposed equation of *SIFs* (Colomb 2005; Liu et al. 2009; Matsumoto et al. 2013). As above mentioned, it seems that the crack growth life of tensile steel member strengthened with CFRP plates have been investigated sufficiently.

On the other hand, edbending fatigue performance of welded joint strengthened with CFRP plates have begun to be investigated. In the previous paper (Matsumoto et al. 2016), the authors investigated the bending fatigue performance of cracked welded joint strengthened with CFRP plates by bending fatigue tests, however, in this research, the effects of width of CFRP plates on bending fatigue performance have not been discussed sufficiently. Therefore, in this research, the effect of the width of CFRP plates on bending fatigue performance is revealed by bending fatigue tests.

Meanwhile, to predict the extended life under bending moment of the cracked welded joint strengthened with CFRP plates, Matsumoto et al. (2017) calculated the *SIF* based on linear fracture mechanics considering various parameters i.e. the widths of CFRP plates, the stiffness of CFRP plates and bonding position. Furthermore, it was shown that the crack growth life of the cracked welded joint strengthened with CFRP plates can be predicted by using calculated *SIF*. However, in the numerical method (Matsumoto el al 2017), the *SIF* was calculated at the surface and depth points of semi-elliptical crack, and surface crack length and crack depth were calculated individually. In this method, the procedure of the crack propagation analysis becomes complicated. Therefore, in this study, procedure of the crack propagation analysis of cracked welded joint reinforced with CFRP plates is simplified. Specifically, in the simplified analysis, crack propagation analysis is conducted by using *SIF* at the surface point and surface crack length is calculated, while crack depth is estimated by using the surface crack length and the aspect ratio of semi-elliptical crack. Finally, the validity of the simplified analysis of crack propagation is clarified, and the effect of width of CFRP plates on bending fatigue performance is predicted.

2 Specimen and Fatigue Test

In the fatigue tests, out-of-plane gusset welded joints fabricated by using JIS-SM490YA, which has guaranteed the yield stress of 355 N/mm^2 and tensile strength of 490 N/mm^2, were prepared (Fig. 1). The specimen was composed of the 12 mm thick gusset plate and the 12 mm thick base plate. The mechanical properties and chemical composition of steel plate are listed in Table 1.

The fatigue test was carried out by using the fatigue testing machine generating a plate bending type of loading, as shown in Fig. 2. A cantilever-type specimen was set on a frame bed and a vibrator was installed on the free end of the base plate. Stress ranges were controlled by the vibration frequency and defined as multiplication of elastic modulus and the initial average strain ranges of gages B1 and B2 (Fig. 1). Stress ratio, *R*, was controlled by the spring installed at the
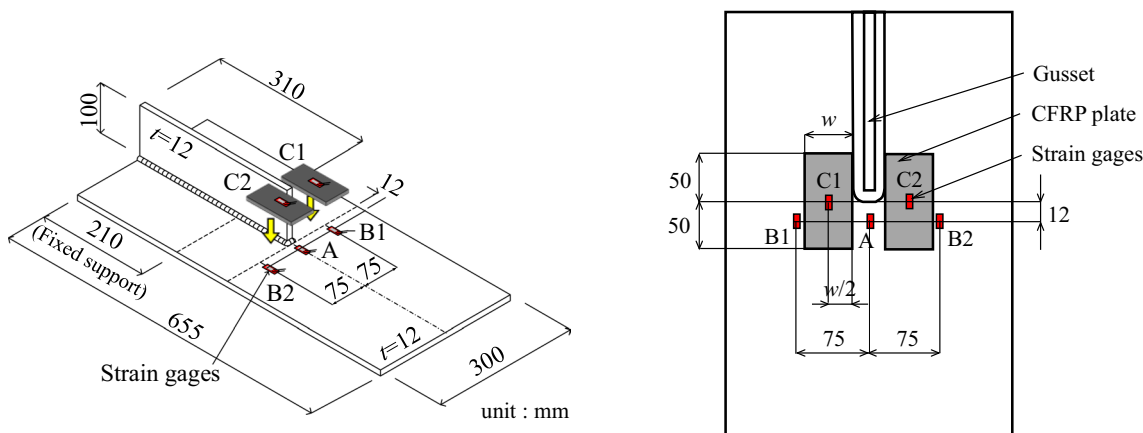

Fig. 1 Test specimen

Table 1 Mechanical properties and chemical composition of the steel plate (SM490Y)

σ_Y (N/mm^2)	σ_b (N/mm^2)	Elongation (%)	Chemical composition (%)			
			C	Si	Mn	S
447	552	21	0.15	0.18	1.41	0.003

Fig. 2 Test set up
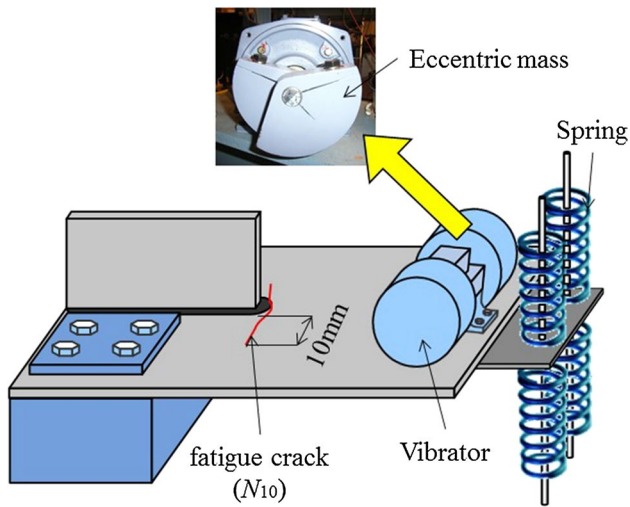

Fig. 3 Variation of strain ranges in the AW_{ref} specimen

free end of the specimen. In this study, stress ratio, R, at the weld toe was controlled as 0 to ignore phenomena of fatigue cack closure.

First, the as-welded specimen was subjected to the cyclic loading until fatigue crack propagated to 10 mm away from the weld toe (N_{10}), as illustrated in Fig. 2. Then, CFRP plates were bonded on the fatigue crack with acrylic resin under unloading condition (Fig. 1), after the bonding surface of the base plate was finished by disk grinder with a roughness number of #100. The longitudinal elastic modus of the CFRP plate is 450 kN/mm^2 and the elastic modulus of acrylic resin is 1.35 kN/mm^2. The CFRP plates used in this study are 2.1 mm in thickness, 100 mm in length and 10 or 25 mm in width. The location of strain gages is shown in Fig. 1. AW specimen indicates the specimen of as-welded condition and N_{10} + CFRP-w10 and N_{10} + CFRP-w25 specimens indicate the specimens repaired by CFRP plates of 10 and 25 mm in width, respectively.

3 Fatigue Test Results

3.1 Variation of Strain Range During Fatigue Test

Variation of the strain ranges during the fatigue tests under stress range of 80 N/mm^2 are shown in Figs. 3 and 4.

Figure 3 is the test results of as-welded specimen (AW_{ref}) in the previous study (Matsumoto et al. 2017), and Fig. 4c is the test results of the specimen reinforced with 50 mm width CFRP plates (N_{10} + CFRP-w50$_{ref}$) in the previous study (Matsumoto et al. 2016). In these figures, the fatigue lives of N_{10} and N_t are plotted as the break lines.

In the AW_{ref} specimen as shown in Fig. 3, the strain range at gage A located in front of the weld toe decreased and the
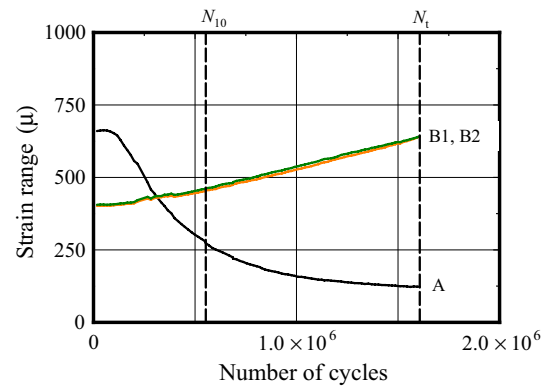
strain ranges at gages B1 and B2 located at the crack tip increased, as the fatigue crack initiated at the weld toe and propagated to the base plate.

In the specimen reinforced with 10 mm width CFRP plates in Fig. 4a, the strain range at gage A decreased and the strain ranges at gages B1 and B2 increased with crack re-propagation as same as the AW_{ref} specimen. Additionally, the strain ranges at gages C1 and C2 located on the CFRP plates increased with fatigue crack re-propagating.

The strain range at the gage C2 sharply dropped at 95,000 cycles, thus it can be assumed that the CFRP plate located at the left side of the gusset was delaminated. After the delamination of the left side CFRP plate, strain ranges at the gages B1 and B2 located at the crack tip increased slightly and the strain range at the gage C1 located at the right side CFRP plate increased greatly. The right side CFRP plate was delaminated at the 0.2 million cycles as the decrease of the strain range of gage C2, and finally fatigue crack was initiated at the back surface of the specimen. The same tendency of the variation of strain ranges in the N_{10} + CFRP-w10 specimen can be seen in the N_{10} + CFRP-w25 specimen and N_{10} + CFRP-w50$_{ref}$ specimen.

Compared with Figs. 4a–c, the strain ranges at gages C1 and C2 located on the CFRP plates increased with decreasing the CFRP width, thus delamination life of CFRP plates decreased with the decreasing the CFRP width.

3.2 S–N Curve

The measured fatigue lives of the tested specimens are summarized in Table 2. Crack growth life from N_{10} to N_t is defined as the number of cycles after fatigue crack propagated 10 mm away from the gusset (N_{10}) until fatigue crack was initiated at the opposite side of the base plate (N_t). The $S–N$ diagram of the fatigue test results is shown in Fig. 5. In Table 2 and Fig. 5, the test results of previous papers (Matsumoto et al. 2016, 2017) are also listed and plotted as AW_{ref} and N_{10} + CFRP-w50$_{ref}$. The
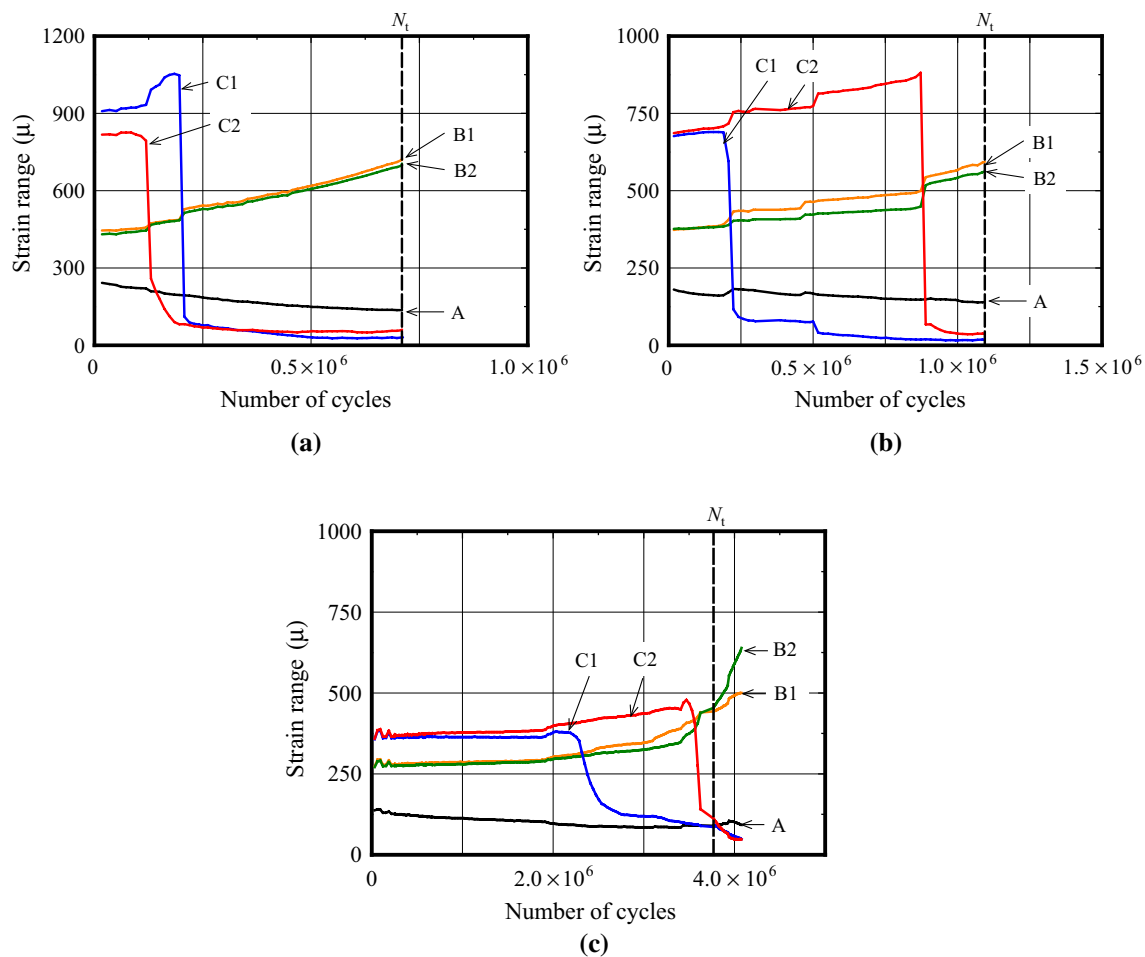
Fig. 4 Variation of strain ranges in the specimen reinforced with CFRP plates. **a** N_{10} + CFRP-w10 specimen, **b** N_{10} + CFRP-w25 specimen, **c** N_{10} + CFRP-w50$_{ref}$ specimen

N_{10} + CFRP-w50$_{ref}$ specimen indicates the crack repaired by CFRP plates of 50 mm in width.

In Fig. 5, the delamination lives of CFRP plates, which are defined as the number of cycles when the strain ranges at the gages C1 and C2 began to decrease, are also plotted as white symbols. As can be seen in Fig. 5, in all specimens, fatigue crack appeared at the back surface of the specimen after the CFRP plates began to be delaminated.

The delamination life of CFRP plates decreased with decreasing the width of CFRP plates, thus the fatigue life N_t becomes shorter with decreasing the width of CFRP plates. Especially, the fatigue lives N_t in the N_{10} + CFRP-w10 and N_{10} + CFRP-w25 specimens are almost same as those in the AW$_{ref}$ specimens, while the N_{10} + CFRP-w50$_{ref}$ specimens showed the significant extended crack growth lives compared with that in the AW$_{ref}$ specimens.

3.3 Observation of the Fracture Surface After Fatigue Test

Figure 6 shows the fracture surfaces after fatigue tests. In all specimens, the N_{10} crack was dye-marked.

As shown in Fig. 6a, in the AW$_{ref}$ specimen, N_{10} crack was propagated in the vertical direction against the gusset plate. In the N_{10} + CFRP-w10 and N_{10} + CFRP-w25 specimens, whose fatigue lives N_t are almost same as the AW$_{ref}$ specimen, the tendency of crack propagation also same as that in the AW$_{ref}$ specimen. On the other hand, in the N_{10} + CFRP-w50$_{ref}$ specimen, whose fatigue life N_t is longer than that in the AW$_{ref}$ specimen, N_{10} crack propagates in the vertical direction and diagonal direction against the gusset plate.

Table 2 Fatigue test results (stress ratio, $R = 0$)

Specimen	State	Stress range (N/mm^2)	Fatigue life $N_{10} \rightarrow N_t (\times 10^4)$
AW-1$_{ref}$	As-welded	80.9	105
AW-2$_{ref}$		101.4	15.4
AW-3$_{ref}$		60.8	198
AW-4$_{ref}$		80.4	58.9
AW-5$_{ref}$		99.9	16.0
AW-6$_{ref}$		124.8	3.96
N_{10}+CFRP-w10	N_{10}crack+CFRP-w10	80.3	71.0
N_{10}+CFRP-w25-1	N_{10}crack+CFRP-w25	78.0	109
N_{10}+CFRP-w25-2		99.4	33.5
N_{10}+CFRP-w50$_{ref}$-1	N_{10}crack+CFRP-w50	57.5	1850
N_{10}+CFRP-w50$_{ref}$-2		57.8	2590
N_{10}+CFRP-w50$_{ref}$-3		80.2	377
N_{10}+CFRP-w50$_{ref}$-4		79.9	411
N_{10}+CFRP-w50$_{ref}$-5		80.7	341
N_{10}+CFRP-w50$_{ref}$-6		101.8	56.8
N_{10}+CFRP-w50$_{ref}$-7		101.5	67.6
N_{10}+CFRP-w50$_{ref}$-8		99.8	123
N_{10}+CFRP-w50$_{ref}$-9		130.0	35.7
N_{10}+CFRP-w50$_{ref}$-10		122.1	26.8
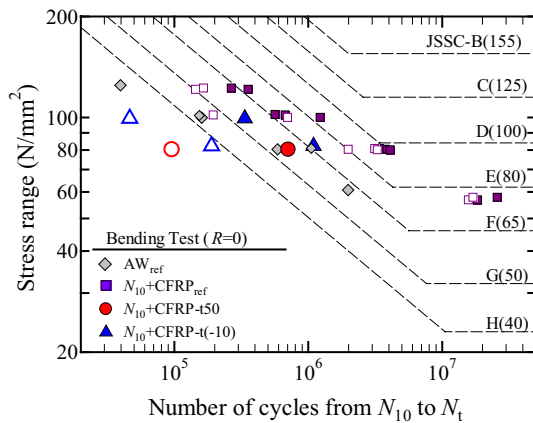
Fig. 5 S–N curve (stress ratio, $R = 0$)

The reason for this difference of the crack propagations between specimens is caused by the difference of the delamination life of CFRP plates. When the delamination life of CFRP plates is longer, the crack propagation in the vertical direction of the fiber direction of CFRP plates can be delayed significantly, and a crack propagates in the diagonal direction of the fiber direction where the reinforced effect is small.

3.4 Relationship Between Crack Length and Number of Cycles

The test results of crack propagation are shown in Figs. 7 and 8. A part of crack depth data is plotted in Figs. 7 and 8, since it is difficult to measure all the data of crack depth. As shown in Fig. 7a, the delay effect in crack propagation for the surface direction becomes higher with the increasing of the CFRP width until delamination of CFRP plates. In the N_{10}+CFRP-w10 and N_{10}+CFRP-w25 specimens, crack growth rate accelerated after delamination of CFRP plates. The same tendency of surface crack propagation can be seen in the specimen tested under stress range of 100 N/mm^2, as shown in Fig. 8a.

In case of the stress range of 80 N/mm^2, while the crack propagations for the depth direction in the N_{10}+CFRP-w10 and N_{10}+CFRP-w25 specimens are both same as that in the AW$_{ref}$ specimen, the N_{10}+CFRP-w50$_{ref}$ specimen showed the delay effect in fatigue crack propagation for the depth direction, as shown in Fig. 7b. In case of stress range of 100 N/mm^2, the delay effect in surface crack propagation becomes higher with increasing width of CFRP plate, as shown in Fig. 8b.
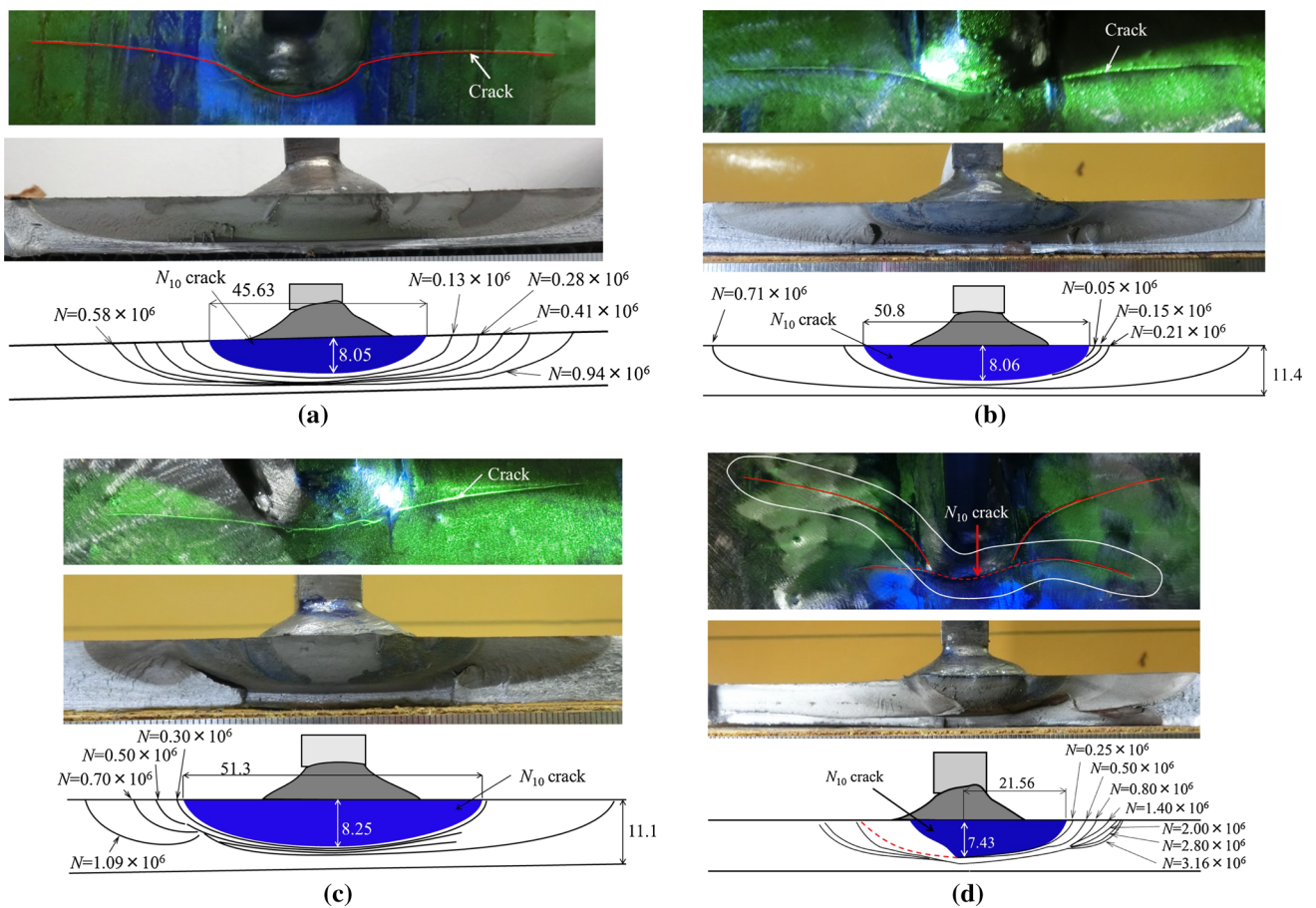
Fig. 6 Fracture surface (stress range $\Delta\sigma = 80$ N/mm^2). **a** AW$_{ref}$ specimen, **b** $N10+$CFRP-$w10$ specimen, **c** $N10+$CFRP-$w25$ specimen, **d** $N10+$CFRP-$w50_{ref}$ specimen
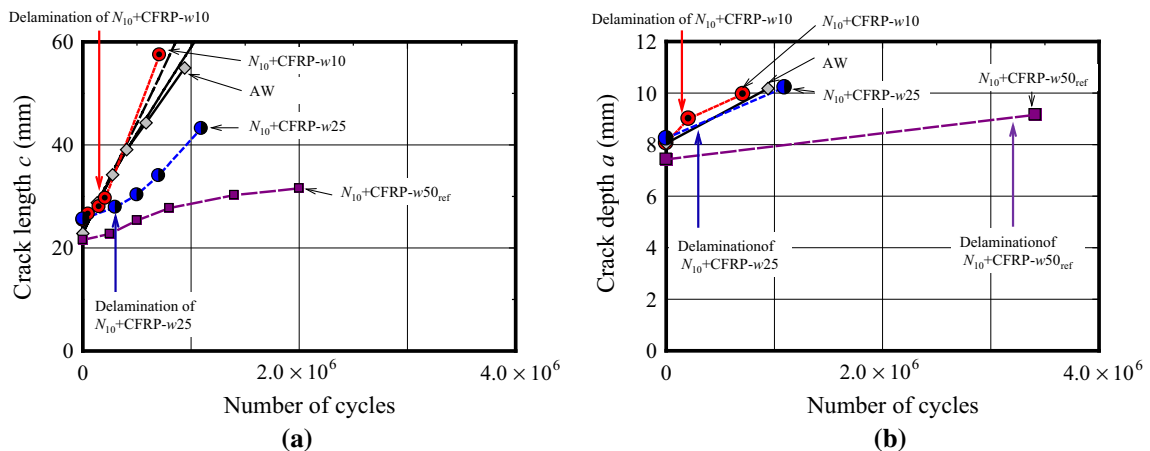

Fig. 7 Test results of crack propagation (stress range $\Delta\sigma = 80$ N/mm^2). **a** Surface direction, **b** depth direction
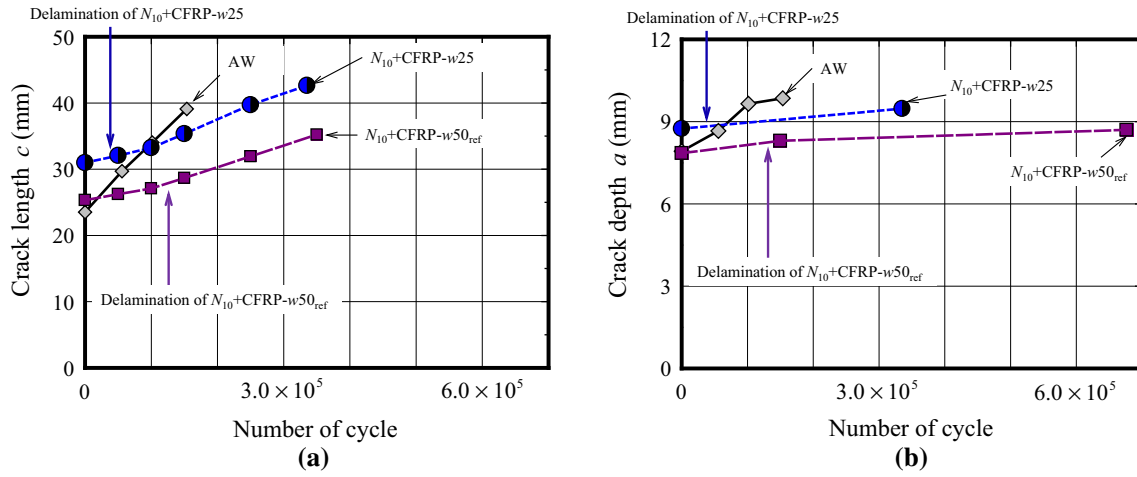
Fig. 8 Test results of crack propagation (stress range $\Delta\sigma = 100$ N/mm^2). **a** Surface direction, **b** depth direction
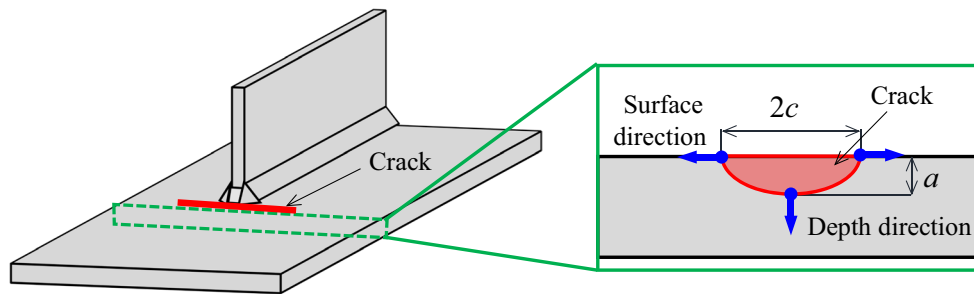

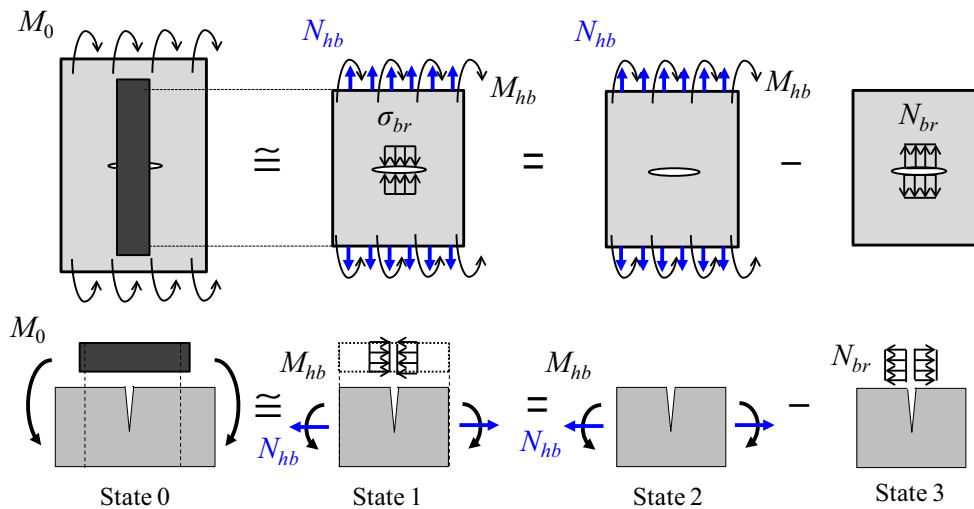**Fig. 9** Assumed crack shape

Fig. 10 Principle of super position

4 Fatigue Crack Propagation Analysis

4.1 Stress Intensity Factor for the Surface Direction

4.1.1 Introduction of Stress Intensity Factor Strengthened with CFRP Plates

In this study, to evaluate the extended fatigue life strengthened with CFRP plates, the *SIF* of semi-elliptical crack strengthened with CFRP plates is estimated by using the proposed equation in the previous study (Matsumoto et al. 2017). In this study, crack shape is assumed as the semi-elliptical crack as shown in Fig. 9.

A schematic view of *SIF* reduction factor by bonding CFRP plates is shown in Fig. 10. When the composite steel and CFRP member is subjected to bending moment M_0, bending moment of M_{hb} and axial load of N_{hb} are applied to the steel plate, since the CFRP bonded section can be regarded as the composite section (State 1 in Fig. 10). On the other hand, since the CFRP plates right on the crack carry the additional axial force, which cannot be transmitted by the crack, the crack opening displacement covered with CFRP plate is reduced compared with unreinforcement state. It can be assumed that the additional axial force distributed to the CFRP plate on the crack, N_{br}, is applied to the crack surface to close the crack (State 1 in Fig. 10). Furthermore, the condition of State 1 can divide into the conditions of States 2 and 3 based on the superposition principle. Thereby, the *SIF* of a crack repaired by bonding CFRP plates, $K_I^{(0)}$, can be estimated by using the *SIF* of State 2, $K_I^{(2)}$, and the *SIF* of State 3, $K_I^{(3)}$.

$$K^{(0)} \cong K^{(1)} = K^{(2)} - K^{(3)} \tag{1}$$

$$K^{(2)} = \left(\sigma_t F_t F_{gweld-t} + \sigma_b F_b F_{gweld-b} \right) \tag{2}$$

$$K^{(3)} = \left(\sigma_{br-t} F_t F_{g-t} + \sigma_{br-b} F_b F_{g-b} \right) \sqrt{\pi b} \tag{3}$$

where b is the crack length ($b = c$ for the surface direction and $b = a$ for the depth direction), σ_t and σ_b are the nominal stresses generated by axial force N_{hb} and bending moment M_{hb}, respectively, σ_{br-t} is the bridging stress generated by additional axial force N_{br}. N_{br} is applied to the centroid of the CFRP plate, thus bending moment M_{br} is applied to the steel plate. σ_{br-b} is the bridging stress generated by additional bending moment M_{br}. F_t and F_b are the correction factors of semi-elliptical surface crack subjected to axial load and bending moment, respectively (correction factors given by Raju-Newman formula). $F_{gweld-t}$ and $F_{gweld-b}$ are the correction factors considering the stress concentration generated at the weld toe subjected to axial load and bending moment, respectively. F_{g-t} and F_{g-b} are the correction factors considering the bridging stress applying to the crack surface under the CFRP plates.

4.1.2 Nominal Stress and Bridging Stress

As shown in Fig. 11, when the steel and CFRP composite member is subjected to bending moment M_0, axial force N_{hb} and bending moment M_{hb} of the steel plate at the intact section can be given by the following equation.

$$N_{hb} = -N_{hp} = -\frac{A_p a_{hp} E_p}{E_b I_{hv}} M_0 \tag{4}$$

$$M_{hb} = \frac{E_b I_{hb}}{E_p I_p + E_b I_{hb}} \{ M_0 + N_{hp}(a_{hp} + a_{hb}) \} \tag{5}$$

where A_{hb} and A_p are the cross-sectional areas of intact steel plate and CFRP plate, respectively; I_{hb} and I_p are the moments of inertia of steel plate in the intact part and CFRP plates, respectively; E_b and E_p are the elastic modulus of steel plate and CFRP plate, respectively; a_{hp} and a_{dp} are the distances from the centroid of the composite member to the center of the steel plate and CFRP plate at the sound part, respectively; $E_b I_{hv}$ is the bending stiffness of the composite member in the intact part, and N_{hp} is the axial force of CFRP plate in the intact part. The nominal stresses σ_t and σ_b can
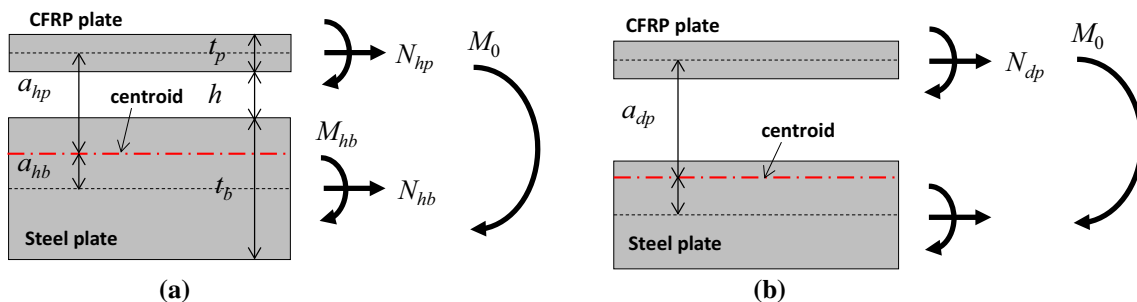

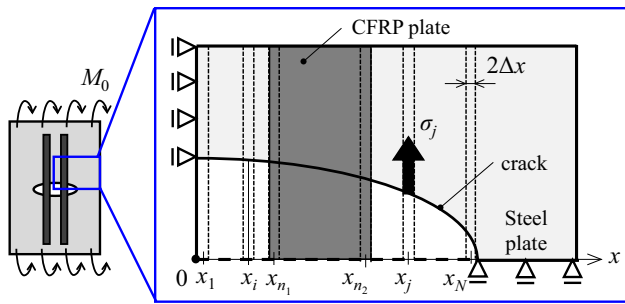**Fig. 11** Distribution of axial load and bending moment. **a** The sound section, **b** The cracked section

Fig. 12 Division model of surface crack

be calculated by $\sigma_t = N_{hp}/A_{hb}$, $\sigma_b = M_{hb}/I_{hp} \cdot t_b/2$, where t_b is the thickness of the intact steel plate.

The additional axial load N_{br} can be expressed by the difference between the axial loads of the CFRP plate in the intact part N_{hp}, and that of the CFRP plate in the cracked part N_{dp}. The axial load of the CFRP plate in the cracked part can be calculated by using composite theory, thus N_{br} can be expressed in the following equation.

$$N_{br} = N_{hp} - N_{dp} \qquad (6)$$

$$N_{dp} = \frac{A_p a_{dp} E_p}{E_b I_{dv}} M_0 \qquad (7)$$

where a_{dp} and $E_b I_{dv}$ are the distance from the centroid of the composite member to the center of CFRP plate in the cracked part, and the bending stiffness of the composite member in the cracked part, respectively.

Since the additional axial load N_{br} is applied to the centroid of the CFRP plate, bending moment M_{br} expressed by the following equation is applied to the steel plate at the cracked part, where h is adhesive thickness.

$$M_{br} = N_{br}\left(\frac{t_p}{2} + h + \frac{t_b}{2}\right) \qquad (8)$$

The bridging stresses σ_{br-t} and σ_{br-b} can be calculated by $\sigma_{br-t} = N_{hp} t_b/A_p t_p$, $\sigma_{br-b} = M_{br} t_b W_b/2 I_{hb} W_p$, where W_b and W_p are the widths of the steel plate and CFRP plate, respectively.

4.1.3 Correction Factor

a. *Correction factor of F_{gweld}*

The correction factor of F_{gweld} considering stress concentration generated at the weld toe can be calculated by the following equation (Albert and Yamada 1977), assuming the crack is divided into N sections as shown in Fig. 12.
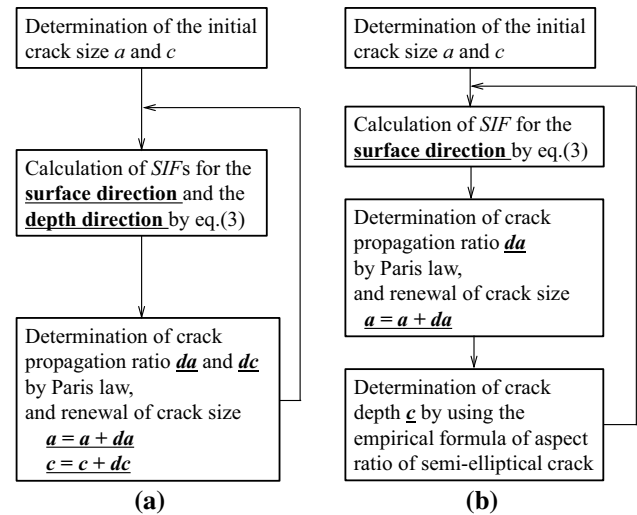

Fig. 13 Calculation flow of crack propagation analysis. **a** Analysis I. (Matsumoto et al. (2017), **b** Analysis II

$$F_{gweld} = \frac{2}{\pi} \sum_{i=1}^{N} (SCF_i \cdot f_g(x_i)) \qquad (9)$$

$$f_g(x_i) = \arcsin\left(\frac{x_i + \Delta x}{b}\right) - \arcsin\left(\frac{x_i - \Delta x}{b}\right) \qquad (10)$$

where SCF_i is the stress concentration factor (SCF) at the section i, Δx is the length of each section. $F_{gweld-t}$ and $F_{gweld-b}$ can be calculated by substituting SCFs under each loading type into Eq. (10).

b. *Correction factor of F_{g-t} and F_{g-b}*

The correction factors of F_{g-t} and F_{g-b} are the factors considering the bridging stress applying to a part of crack surface. Thus, F_{g-t} and F_{g-b} at the surface point can be calculate by the following equation, when the SCFs under each loading type is substituted into Eq. (11).

$$F_g = \frac{2}{\pi} \sum_{i=n_1}^{n_2} (SCF_i \cdot f_g(x_i)) \qquad (11)$$

where n_1 and n_2 is the first and last section where CFRP plates are bonded, as shown in Fig. 12.

In the previous study (Matsumoto et al. 2017), F_{g-t} and F_{g-b} at the depth point can be calculate by the following equation, assumed that the ratio of the SIFs subjected to the non-uniform stress and uniform stress for the depth direction is equal to the ratio of the crack center displacements subjected to the non-uniform stress and uniform stress $\delta_A{}'$ and $\delta_B{}'$.

$$F_g = \frac{\delta_A'}{\delta_B'} \qquad (12)$$

$$\delta'_A = \sum_{j=n_1}^{n_2} \{SCF_i \cdot g(x_1, x_j)\} \tag{13}$$

$$\delta'_B = \sum_{j=1}^{N} \{SCF_i \cdot g(x_1, x_j)\} \tag{14}$$

$$g(x_i, x_j) = g'(-x_i, x_j) + g'(x_i, x_j) \tag{15}$$

$$g'(x_i, x_j) = \frac{2}{\pi E_b} \left[(b_2 - x_i) \cosh^{-1} \left(\frac{c^2 - b_2 x_i}{c |b_2 - x_i|} \right) \right.$$
$$- (b_1 - x_i) \cosh^{-1} \left(\frac{c^2 - b_1 x_i}{c |b_1 - x_i|} \right)$$
$$\left. + \sqrt{c^2 - x_i^2} \left\{ \sin^{-1} \left(\frac{b_2}{c} \right) - \sin^{-1} \left(\frac{b_1}{c} \right) \right\} \right]$$
$$\times \left\{ \frac{\sin^{-1} B_2 - \sin^{-1} B_1}{\sin^{-1} (b_2/c) - \sin^{-1} (b_1/c)} \right\} \tag{16}$$

$$B_k = \sin \left(\pi b_k / W_b \right) / \sin \left(\pi c / W_b \right) \tag{17}$$

$$b_1 = x_j - \Delta x \tag{18}$$

$$b_2 = x_j + \Delta x \tag{19}$$

4.2 Crack Propagation Analysis

To evaluate the crack growth life of cracked welded joint strengthened with CFRP plates under bending moment, two types of crack propagation analyses were conducted. The calculation procedures of crack propagation analysis are shown in Fig. 13.

In the Analysis I proposed in the previous paper (Matsumoto et al. 2017), after determination of the initial crack sizes a and c, the SIFs are calculated at the surface and depth points of the semi-elliptical crack. The crack propagation da and dc are calculated individually by using the calculated SIF and Paris law:

$$\frac{db}{dN} = C \left(\Delta K^m - \Delta K_{th}^m \right) \tag{20}$$

where C and m are material properties, N is the number of cycles, and ΔK_{th} is the threshold stress intensity factor range. In this study, ΔK_{th} is assumed as 0, and material properties of C and m are determined by the applying the least square method to the relationship between db/dN and ΔK given by the AW_{ref} specimen. The determined material properties are $C = 2.865 \times 10^{-13}$ and $m = 2.854$. The SIF in the AW specimen is calculated by multiplying Raju-Newman formula by F_{gweld} expressed by Eq. (9), and the SIF strengthened with CFRP plates is calculated by using Eq. (3).

In the Analysis II, after determination of initial crack sizes a and c, the SIF is calculated only at the surface point, and the crack propagation ratio da is calculated by using Paris law. After the renewal of the crack length a, crack depth c is calculated by using the empirical formula of aspect ratio of semi-elliptical crack in the following equation (MORI and MIKI 1995).

$$\frac{a}{2c} = \frac{1}{2 + 2c/t_b} \tag{21}$$

The calculation procedure in the Analysis II is more simple than that in the Analysis I, since the Equation of the SIF for the depth direction [Eq. (12)] is complicated.

4.3 Estimated Results of Crack Growth Life of Cracked Welded Joint Strengthened with CFRP Plates Under Bending Moment

Figures 14, 15, 16 and 17 show the estimated results of crack growth life of cracked welded joint strengthened with CFRP plate under bending moment by the Analyses I and II. As shown in Fig. 14, the delay effect in fatigue crack propagation for the surface direction can be evaluated accurately in the all specimens until delamination of CFRP plates. Furthermore, the estimate results by Analysis II are almost same as those by Analysis I. The same tendency can be seen in the specimen tested under stress range of $\Delta\sigma = 100$ N/mm^2, as shown in Fig. 16.

In the depth direction, the estimated crack growth rate by Analysis II tend to be smaller than that by Analysis I, as shown in Fig. 15. The reason of this is assumed that the estimated SIF by Eq. (3) tends to be larger than the calculated SIF by the finite element analysis (Matsumoto et al. 2017). The effect of the width of the CFRP plate on crack growth rate can be simulated in both analysis procedures. However, the accuracy of the estimated results cannot be discussed, since the tested data are not sufficient. This tendency also can be seen in the specimen tested under stress range of $\Delta\sigma = 100$ N/mm^2, as shown in Fig. 17.

Therefore, it can be concluded that the Analyses I and II can evaluate accurately the surface crack growth giving strong influence on extended fatigue life of semi-elliptical crack strengthened with CFRP plates under bending moment, thus the analysis by using the SIF for the surface direction and the empirical formula of the aspect ratio of semi-elliptical crack is effective for the prediction of crack growth life of cracked welded joint strengthened with CFRP plates under bending moment.
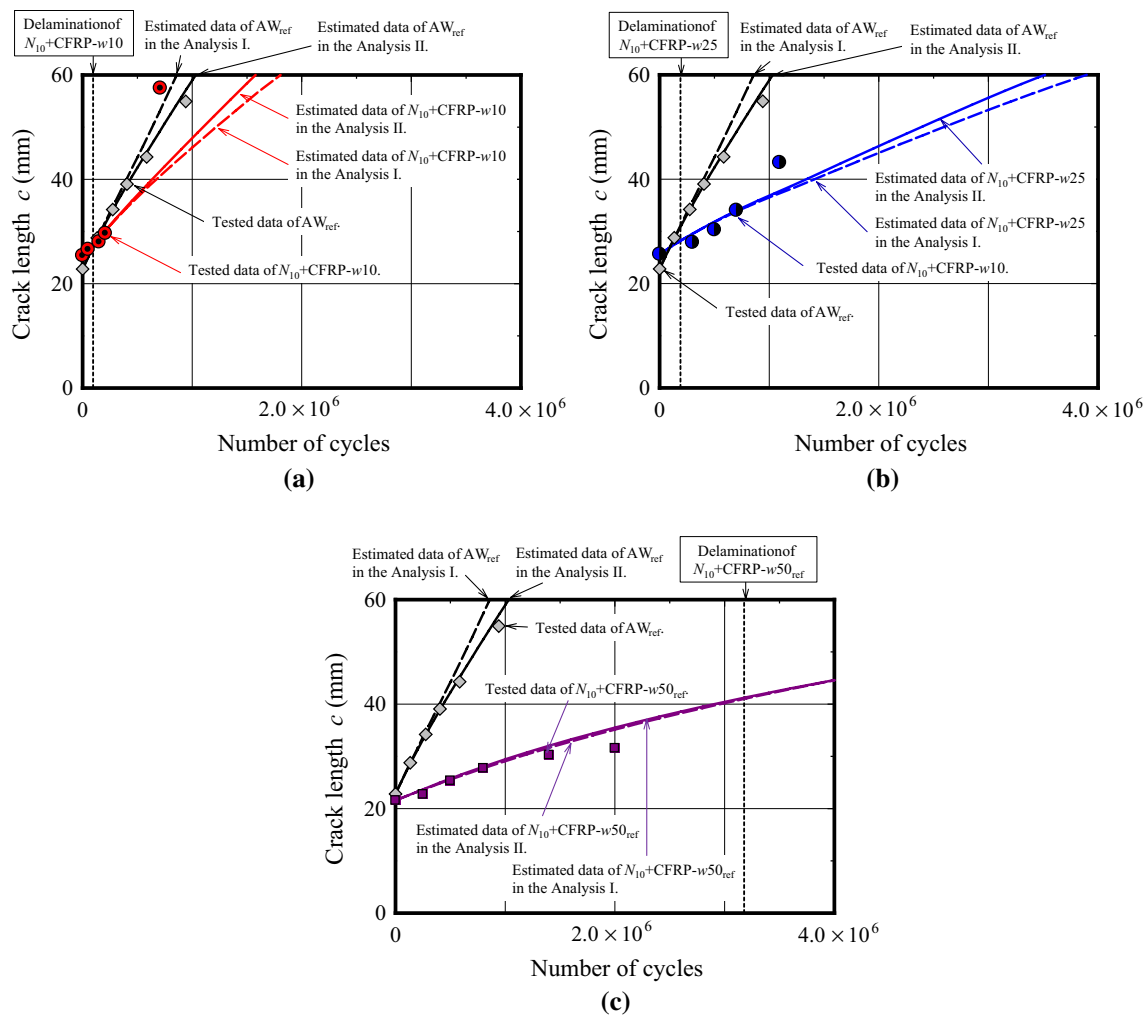
Fig. 14 Estimated results of crack propagation for the surface direction (stress range $\Delta\sigma = 80$ N/mm^2). **a** $N_{10}+$CFRP-$w10$ specimen, **b** $N_{10}+$CFRP-$w25$ specimen, **c** $N_{10}+$CFRP-$w50_{\text{ref}}$ specimen

5 Conclusions

In this study, the effect of the width of CFRP plates on crack growth life under bending moment was clarified by bending fatigue tests, and extended fatigue life is evaluated by using the empirical formula of the aspect ratio of semi-elliptical crack and the *SIF* for the surface direction estimated based on the linear fracture mechanics. The main conclusions are as follows:

1. The specimen strengthened with 50 mm width of CFRP plates showed the significant fatigue life extension compared with that in the as-welded specimen. However, the specimen strengthened with 10 or 25 mm width of CFRP plates showed almost same crack growth life of the as-welded specimen, since the delamination life of CFRP

plates is shorter than that in the specimen strengthened with 50 mm width of CFRP plates.

2. The delay effect in fagtigue crack propagation for the surface direction becomes higher with increasing width of CFRP plates until the delamination of CFRP plates, and crack growth rate accelerated after delamination of CFRP plates.

3. In the specimen reinforced with 50 mm width of CFRP plates, the fatigue crack re-propagated in the diagonal direction and vertical direction against the gusset plate, while the fatigue crack re-propagated in the vertical direction of the gusset plate in the specimen strengthened with 10 or 25 mm width of CFRP plates. This difference is caused by the difference of the delamination life of CFRP plates.

4. The crack growth life can be evaluated accurately by the analysis using the empirical formula of the aspect
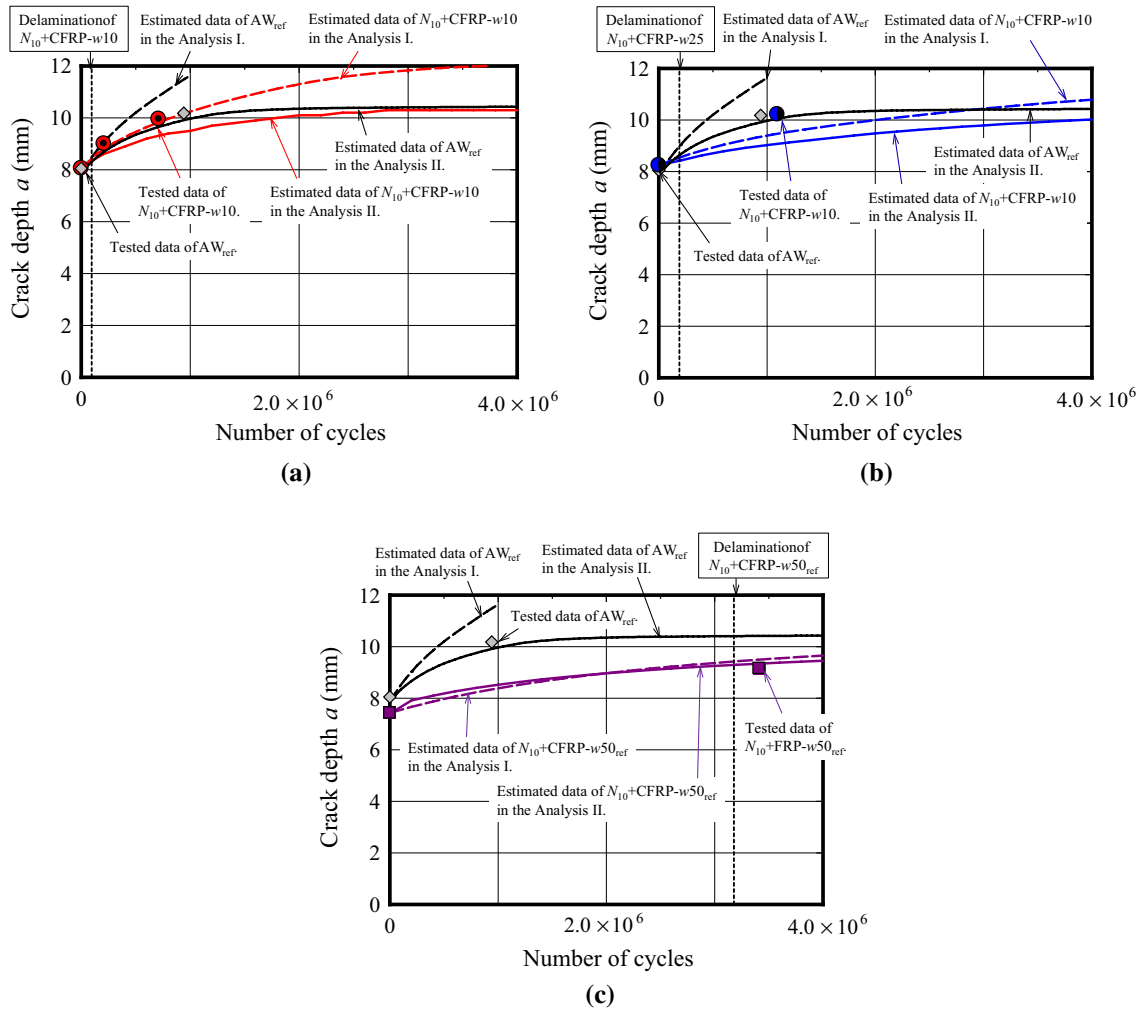
Fig. 15 Estimated results of crack propagation for the depth direction (stress range $\Delta\sigma=80$ N/mm^2). **a** $N_{10}+$CFRP-w10 specimen, **b** $N_{10}+$CFRP-w25 specimen, **c** $N_{10}+$CFRP-w50$_{ref}$ specimen
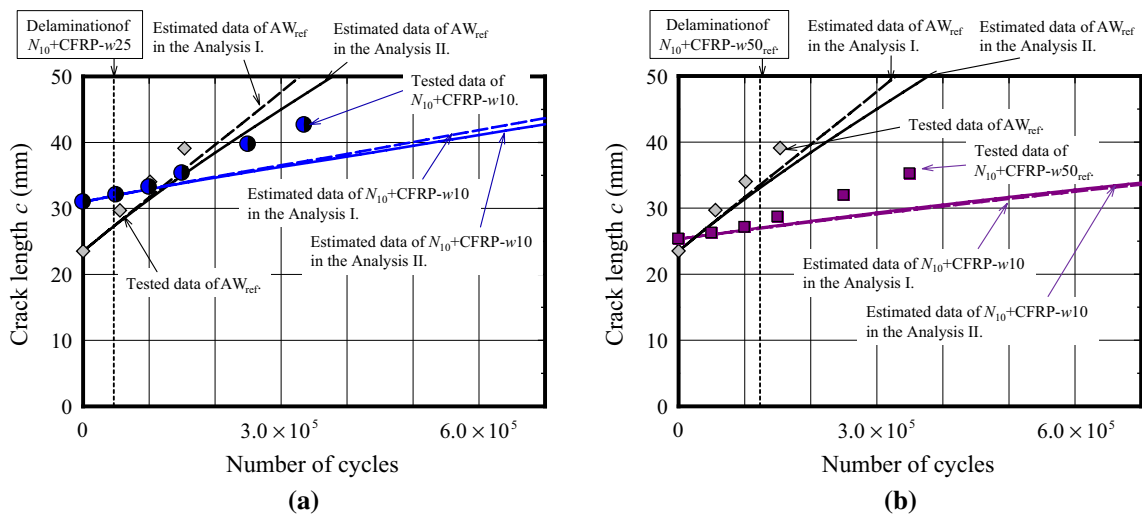

Fig. 16 Estimated results of crack propagation for the surface direction (stress range $\Delta\sigma=100$ N/mm^2). **a** $N_{10}+$CFRP-w25 specimen, **b** $N_{10}+$CFRP-w50$_{ref}$ specimen
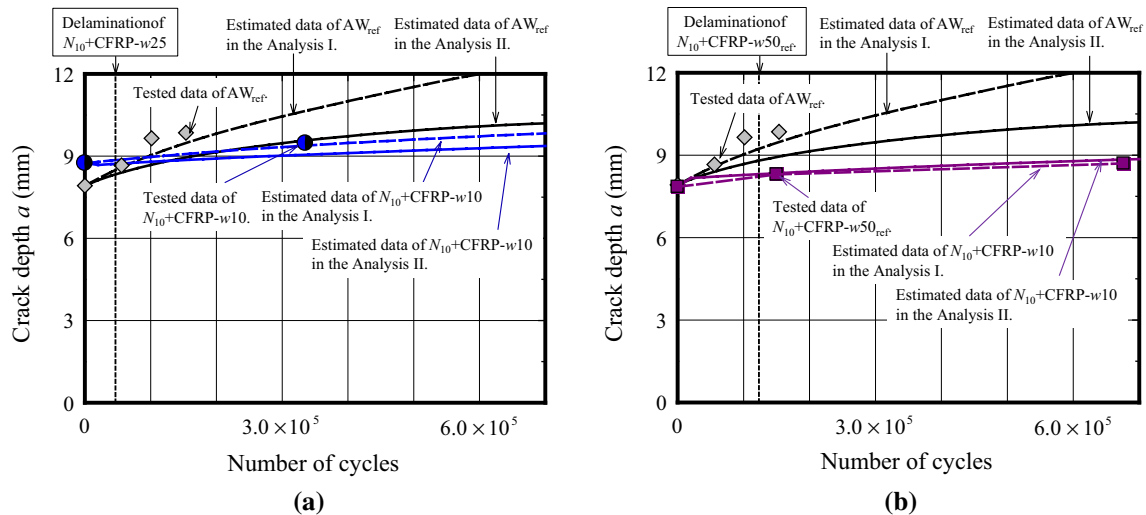
Fig. 17 Estimated results of crack propagation for the depth direction (stress range $\Delta\sigma = 100$ N/mm^2). **a** N_{10} + CFRP-$w25$ specimen, **b** N_{10} + CFRP-$w50_{\text{ref}}$ specimen

ratio of semi-elliptical crack and the *SIF* for the surface direction estimated based on the linear fracture mechanics, when the CFRP plates are effectively working. Furthermore, the estimated result of the simple procedure is almost same as the estimated results of the previous method in which analysis is conducted by using the *SIF* at the surface and depth points individually. Therefore, it is clarified that the simple analysis procedure proposed in this paper is effective for the evaluation of the crack growth life of cracked welded joint strengthened with CFRP plates under bending moment.

References

Albrecht, P., & Yamada, K. (1977). Rapid calculation of stress intensity factors. *Journal of the Structural Division-ASCE, Proceeding Paper 12742, 103*(ST2), 377–389.

Chacon, A., Chajes, M. J., Richardson, D., & Wenczel, G. (2004). Applications of advanced composites to steel bridges a case study on the Ashland Bridge (Delaware-USA). In *Proceedings of the 4th international conference on advanced composite materials in bridges and structures* (p. 8). Calgary, Canada.

Colombi, P. (2005). Plasticity induced fatigue crack growth retardation model for steel elements reinforced by composite patch. *Theoretical and Applied Fracture Mechanics, 43,* 63–76.

Colombi, P., Fava, G., & Sonzogni, L. (2015). Fatigue crack growth in CFRP-strengthened steel plates. *Composites: Part B, 72,* 87–96.

Liu, H., Xiao, Z., Zhao, X. L., & Al-Mahaidi, R. (2009). Prediction of fatigue life for CFRP-strengthened steel plates. *Thin Welled Structures, 47*(10), 1069–1077.

Matsumoto, R., Ishikawa, T., Hattori, A., & Kawano, H. (2013). Stress intensity factor of a cracked steel plate repaired with patch plates. *Journal of Structural Engineering A, 59A,* 798–807. **(in Japanese)**.

Matsumoto, R., Ishikawa, T., Takemura, M., Hiratsuka, Y., & Kawano, H. (2016). Extending fatigue life of out-of-plane gusset joint by bonding CFRP plates under bending moment. *International Journal of Steel Structure, 16*(4), 1319–1327.

Matsumoto, R., Komoto, T., Ishikawa, T., Hattori, A., & Kawano, H. (2017). The effect of plate bonding method on reduction of stress intensity factor of cracked out-of-plane gusset joint subjected to bending moment. *Japan Society of Civil Engineering 2017 Annual Meeting, I-114,* 227–228. **(in Japanese)**.

Mori, T., & Miki, C. (1995). Aspect ratios of surface fatigue cracks originated in fillet welded joints. *Journal of Structural Engineering A, 41A,* 829–838. **(in Japaneses)**.

National Research Council—Advisory Committee on Technical Recommendations for Construction. (2007). *Guidelines for the design and construction of externally bonded FRP systems for strengthening existing structures*, CNR-DT 202/2005.

Phares, B. M., Wipf, T. J., Klaiber, F. W., Abu-Hawash, A., & Lee, Y. S. (2003). Strengthening of steel girder bridges using FRP. In *Proceedings of the 2003 mid-continent transportation research symposium*.

Roach, D., Rackow, K., Delong, W., & Franks, E. (2008). In-situ repair of steel bridges using advanced composite materials, international bridge and structure management. In *10th international conference on bridge and structure management, transportation research circular E-C128* (pp. 269–285).

Wang, H. T., Wu, G., & Wu, Z. S. (2013). Effect of FRP configurations on the fatigue repair effectiveness of cracked steel plates. *Journal of Composites for Construction, ASCE, 18*(1), 04013023.

Ye, H. W., König, C., Ummenhofer, T., Qiang, S. Z., & Plum, R. (2010). Fatigue performance of tension steel plates strengthened with prestressed CFRP laminates. *Journal of Composites for Construction, ASCE, 14*(5), 609–615.